ADAPTIVE BEAMFORMING BY CONSTRAINED PARALLEL PROJECTION IN THE PRESENCE OF SPATIALLY-CORRELATED INTERFERENCES

Masahiro YUKAWA and *Isao YAMADA*

Dept. of Communications and Integrated Systems (S3-60),
Tokyo Institute of Technology, Tokyo 152-8552, JAPAN
E-mails: {masahiro,isao}@comm.ss.titech.ac.jp

ABSTRACT

The contribution of this paper is twofold. We first clarify geometrically an inherent difference in convergence speed between two adaptive algorithms, projected-NLMS (PNLMS) and constrained-NLMS (CNLMS), both of which are widely used for linearly constrained adaptive filtering problems. A simple geometric interpretation suggests that CNLMS converges faster than PNLMS especially in the challenging situations of the adaptive beamforming where there exist spatially-correlated interferences (i.e., interferences that have small angular separation with the desired signal). To enhance the advantage of CNLMS in convergence speed while keeping linear computational complexity, we then propose an efficient adaptive beamformer that utilizes multiple data at each iteration by extending the constrained parallel projection algorithm to complex cases. The simulation results demonstrate that the proposed beamformer exhibits even faster convergence than the constrained affine projection algorithm (CAPA) as well as CNLMS.

1. INTRODUCTION

The *linearly constrained adaptive filtering problem* has received considerable attention due to its important applications such as adaptive beamforming, multiuser detection in CDMA, and spectral estimation [1–9]. We focus on the adaptive beamforming application, although similar discussion could be possible for other applications. In [10], it is reported that the signal to interference-plus-noise ratio (SINR) performance of *minimum variance beamformer* is affected by spatial/temporal-correlation[1] between the desired and interfering signals as well as signal to noise ratio (SNR), interference to noise ratio (INR) etc. Although an extensive amount of studies has been done to deal with the temporally-correlated case (see, e.g., [11]), few studies have been reported in the spatially-correlated case [12]. This paper provides a new insight to the challenging spatially-correlated situations.

We shed light on the least mean square (LMS) type approach to the adaptive beamforming, because it enjoys notable advantages of linear computational complexity and self-correcting feature [1] (see [7] for other approaches). To raise the convergence speed of the method in [1], several improved versions have been proposed [4, 5, 9]. On the other hand, a related algorithm has been independently proposed for the multiuser detection problem in CDMA [2, 3], and its improved version is also proposed in [8] (an extension of the method in [8] to complex-valued signals is presented in [13]). From a geometric viewpoint, we classify the existing LMS type approaches into two families: *embedded-constraint type* [4, 5, 9] and *non-embedded-constraint type* [1–3, 8, 13] (see [9] for this classification). Respective typical examples of embedded and non-embedded families are *constrained NLMS (CNLMS)* [4] and *projected NLMS (PNLMS)* [3], both of which are widely used in linearly constrained adaptive filtering applications due to their computational simplicity and reasonable convergence property. Hence, it is of great interest to investigate the difference in convergence speed between CNLMS and PNLMS.

In this paper, we first provide a desirable strategy to the adaptive beamforming in spatially-correlated cases. By a simple geometric interpretation, a great advantage of CNLMS over PNLMS in convergence speed can be expected especially in the presence of spatially-correlated interferences. (This feature is confirmed in our extensive simulations, one of which is shown in Fig. 1.) This observation motivates us to explore a more efficient algorithm in the embedded-constraint family, to which CNLMS belongs. To enhance the advantage of CNLMS, we propose a promising embedded-constraint adaptive beamformer, which utilizes multiple data at each iteration by extending the constrained parallel projection algorithm [9] to complex cases. Simulation results demonstrate that the proposed algorithm successfully accelerates convergence speed while keeping linear computational complexity (see Sec. 4).

[1]The spatial correlation is related to angular separation, and the temporal correlation is also referred to as coherence (see, e.g., [11]).

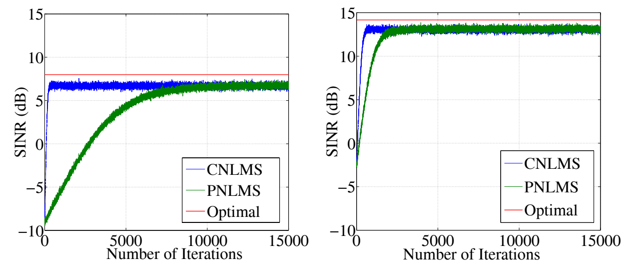

(a) spatially-correlated (b) spatially-uncorrelated

Fig. 1. Performance of the CNLMS and PNLMS algorithms.

2. LINEARLY CONSTRAINED ADAPTIVE BEAMFORMING PROBLEM

We consider narrowband beamforming scenarios with N antenna elements of uniform linear array (ULA) [7] (see Fig. 2). Throughout the paper, $\mathcal{H}_{\mathbb{R}} := \mathbb{R}^{2N}$ and $\mathcal{H}_{\mathbb{C}} := \mathbb{C}^N$ denote real and complex Hilbert spaces equipped with inner products $\langle \boldsymbol{x}, \boldsymbol{y}\rangle := \boldsymbol{x}^T\boldsymbol{y}$, $\forall \boldsymbol{x}, \boldsymbol{y} \in \mathcal{H}_{\mathbb{R}}$, and $\langle \boldsymbol{x}, \boldsymbol{y}\rangle := \boldsymbol{x}^H\boldsymbol{y}$, $\forall \boldsymbol{x}, \boldsymbol{y} \in \mathcal{H}_{\mathbb{C}}$, respectively (superscripts T, H: *transposition, Hermitian transposition*, respectively). We can define a bijective mapping between $\mathcal{H}_{\mathbb{R}}$ and $\mathcal{H}_{\mathbb{C}}$, as shown in Sec. 3.2. Let $(q_j(k))_{k\in\mathbb{N}^*} \subset \mathbb{C}$ [$\mathbb{N}^* := \mathbb{N} \setminus \{0\}$], for $j = 0, 1, \cdots, J$, be the sequence of jth transmitted signals, and $\boldsymbol{s}_j \in \mathcal{H}_{\mathbb{C}}$ ($j = 0, 1, \cdots, J$) the corresponding steering vectors, where the 0th signal is the signal of interest (SOI) and the others interferences. Here, the steering vector is defined as $\boldsymbol{s}_j := \boldsymbol{s}(\theta_j, d, \lambda) := \frac{1}{\sqrt{N}}[1, e^{2\pi i d \cos\theta_j/\lambda}, \cdots, e^{2\pi i (N-1) d \cos\theta_j/\lambda}]^T \in \mathcal{H}_{\mathbb{C}}$, $\forall j \in \{0, 1, \cdots, J\}$, where θ_j stands for the direction of arrival (DOA) of the jth signal, d the distance between two adjacent elements of ULA, and λ the wavelength of the impinging signals ($i := \sqrt{-1}$). Let $(\boldsymbol{n}(k))_{k\in\mathbb{N}^*} \subset \mathcal{H}_{\mathbb{C}}$ be the sequence of additive noise vectors. The received signal vector at the ULA is expressed as $\boldsymbol{y}(k) := [y_1(k), y_2(k), \cdots, y_N(k)]^T := q_0(k)\boldsymbol{s}_0 + \sum_{j=1}^{J} q_j(k)\boldsymbol{s}_j + \boldsymbol{n}(k) \in \mathcal{H}_{\mathbb{C}}$, where $y_n(k) \in \mathbb{C}$,

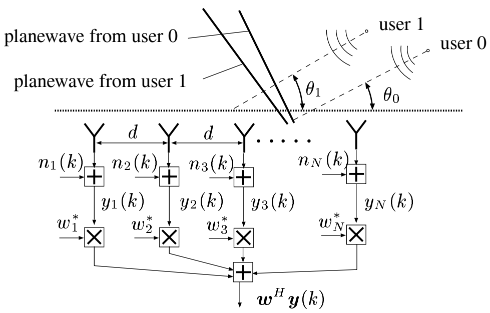

Fig. 2. Uniform linear array with narrowband adaptive beamformer.

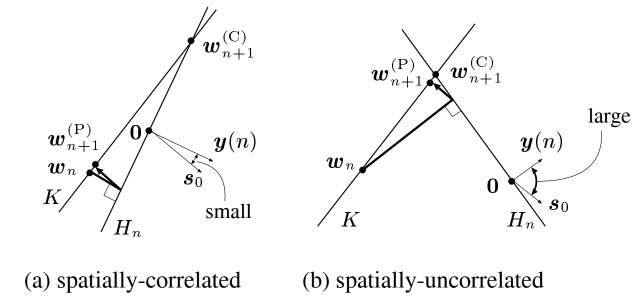

Fig. 3. A geometric interpretation: CNLMS versus PNLMS under two different cases. $\boldsymbol{s}_0$ and $\boldsymbol{y}(n)$ are the normal vectors of K and H_n, respectively. We let $\boldsymbol{w}_n^{(\mathrm{C})} = \boldsymbol{w}_n^{(\mathrm{P})} = \boldsymbol{w}_n$ for comparison.

$\forall n \in \{1, 2, \cdots, N\}$, denotes the received signal at the nth antenna at the kth snapshot.

Throughout, we assume that the available information is the received signal $(\boldsymbol{y}(k))_{k\in\mathbb{N}^*}$ and $\boldsymbol{s}_0$. Given $K(\boldsymbol{A}, \boldsymbol{b}) := \{\boldsymbol{z} \in \mathcal{H}_{\mathbb{C}} : \boldsymbol{A}^H\boldsymbol{z} = \boldsymbol{b}\}$ ($\boldsymbol{A} \in \mathbb{C}^{N\times L}$, $\boldsymbol{b} \in \mathbb{C}^L$), the *linearly constrained narrowband beamforming problem* is stated as follows:

$$\text{find } \boldsymbol{w}_{\text{opt}} \in \arg\min_{\boldsymbol{z}\in K(\boldsymbol{A},\boldsymbol{b})} \boldsymbol{z}^H\boldsymbol{R}_{\boldsymbol{y}}\boldsymbol{z}, \tag{1}$$

where $\boldsymbol{R}_{\boldsymbol{y}} := E\{\boldsymbol{y}(k)\boldsymbol{y}(k)^H\} \in \mathbb{C}^{N\times N}$ is the autocorrelation matrix of $\boldsymbol{y}(k)$ ($E\{\cdot\}$: *expectation*). In the following, for simplicity, we focus on a special case $\boldsymbol{A} = \boldsymbol{s}_0$ and $\boldsymbol{b} = 1$ (see [7, Sec. 6.7.1] for other typical constraints), where the constraint set is given by

$$K := K(\boldsymbol{s}_0, 1) = \{\boldsymbol{z} \in \mathcal{H}_{\mathbb{C}} : \langle \boldsymbol{s}_0, \boldsymbol{z}\rangle = 1\}. \tag{2}$$

In this case, the optimal distortionless beamformer is given by $\boldsymbol{w}_{\text{CB}} := \boldsymbol{w}_{\text{opt}} = (\boldsymbol{R}_{\boldsymbol{y}}^{-1}\boldsymbol{s}_0)/(\boldsymbol{s}_0^H\boldsymbol{R}_{\boldsymbol{y}}^{-1}\boldsymbol{s}_0)$, which is called the *minimum power distortionless response (MPDR) beamformer* or the *Capon Beamformer (CB)* [7]. The goal is to well-approximate the optimal beamformer $\boldsymbol{w}_{\text{opt}}$ with limited observable snapshots. Note that the set K is a *hyperplane* referred to as an absolute (or a hard) constraint.

3. A NEW INSIGHT INTO ADAPTIVE BEAMFORMING IN SPATIALLY-CORRELATED CASES

A basic principle of the CLMS [1], CNLMS [4] and PNLMS [3] has been demonstrated geometrically in [6]. To clarify further the feature of CNLMS and PNLMS, we first provide a different geometric interpretation by focusing two distinctive situations in adaptive beamforming: the desired and interfering signals are (a) spatially-correlated and (b) spatially-uncorrelated. The interpretation gives a reasonable support to the interesting phenomenon observed in Fig. 1. We then present an efficient set-theoretic adaptive beamformer, which is based on a parallel projection onto certain closed convex sets. Also we present an efficient formula to compute the projections onto those convex sets.

3.1. Convergence Speed of CNLMS and PNLMS

Let us first present the CNLMS [4] and PNLMS [3] algorithms in a complex-valued vector form below, although the algorithms are originally proposed in a real-valued vector form (A complex-valued vector expression of the constrained LMS (CLMS) algorithm [1] is given in [14]). Given a non-empty closed convex subset S in any Hilbert space $\mathcal{H}$ and a vector $\boldsymbol{a} \in \mathcal{H}$, $P_S(\boldsymbol{a}) \in S$ denotes the *projection* of $\boldsymbol{a}$ onto S; i.e., $\mathrm{d}(\boldsymbol{a}, S) := \min_{\boldsymbol{z}\in S} \|\boldsymbol{a} - \boldsymbol{z}\| = \|\boldsymbol{a} - P_S(\boldsymbol{a})\|$. The CNLMS and PNLMS algorithms are given as follows.

Algorithms. Let K be a linear constraint set and $(H_n)_{n\in\mathbb{N}^*}$ a sequence of hyperplanes defined by observed data. Given an initial vector $\boldsymbol{w}_0^{(\mathrm{C})} = \boldsymbol{w}_0^{(\mathrm{P})} = \boldsymbol{s}_0 \in K$, the CNLMS and PNLMS algorithms generate respectively sequences $(\boldsymbol{w}_n^{(\mathrm{C})})_{n\in\mathbb{N}^*} \subset K$ and $(\boldsymbol{w}_n^{(\mathrm{P})})_{n\in\mathbb{N}^*} \subset K$ as

$$\text{CNLMS: } \boldsymbol{w}_{n+1}^{(\mathrm{C})} := \boldsymbol{w}_n^{(\mathrm{C})} + \lambda_n \left[P_{H_n\cap K}(\boldsymbol{w}_n^{(\mathrm{C})}) - \boldsymbol{w}_n^{(\mathrm{C})}\right],$$

$$\text{PNLMS: } \boldsymbol{w}_{n+1}^{(\mathrm{P})} := P_K\left\{\boldsymbol{w}_n^{(\mathrm{P})} + \lambda_n \left[P_{H_n}(\boldsymbol{w}_n^{(\mathrm{P})}) - \boldsymbol{w}_n^{(\mathrm{P})}\right]\right\},$$

$\forall n \in \mathbb{N}^*$, where $\lambda_n \in [0, 2]$ is the step size.

As a simple example, $H_n := \{\boldsymbol{z} \in \mathcal{H}_{\mathbb{C}} : \langle \boldsymbol{y}(n), \boldsymbol{z}\rangle = 0\}$, $\forall n \in \mathbb{N}^*$, is used in Fig. 1 as in[2] [3] and [4]. A natural question would be which algorithm is better. The remaining of this subsection is devoted to this issue.

Fig. 1 shows the results of simulations under $d/\lambda = 0.5$ and $J = 2$ interferences, where the signals arrive from $\theta_0 = 0^\circ$, $\theta_1 = 50^\circ$ and (a) $\theta_2 = 15^\circ$, (b) $\theta_2 = 30^\circ$. Namely, the 2nd interference in (a) has smaller angular separation with SOI than the one in (b). The powers of both interferences are 10 times greater than the one of SOI. The number of antennas is set to (a) $N = 15$ for better SINR performance and (b) $N = 10$. The noise process $(\boldsymbol{n}(k))_{k\in\mathbb{N}^*}$ is a complex vector i.i.d. Gaussian process with $E\{\boldsymbol{n}(k)\} = \mathbf{0}$, $\forall k \in \mathbb{N}^*$, correlation matrix $\boldsymbol{R}_n := E\{\boldsymbol{n}(k)\boldsymbol{n}^H(k)\} = \sigma_n^2\boldsymbol{I}_N$, $\forall k \in \mathbb{N}^*$, and SNR $= 15$ dB. For PNLMS, the step size is set to $\lambda_n = 0.005$, $\forall n \in \mathbb{N}^*$, as a reference, and the step size for CNLMS is tuned [(a) $\lambda_n = 0.05$, (b) $\lambda_n = 0.012$, $\forall n \in \mathbb{N}^*$] so as to achieve the same steady-state performance as PNLMS. The output SINR is calculated by averaging over 500 realizations (see also [9]).

We define the *spatial-correlation* between two signals with their associated steering vectors $\boldsymbol{a}$ and $\boldsymbol{b}$ as $\cos(\boldsymbol{a}, \boldsymbol{b}) := \langle \boldsymbol{a}, \boldsymbol{b}\rangle_R / (\|\boldsymbol{a}\| \cdot \|\boldsymbol{b}\|)$; $(z)_R$ stands for the real part of $z \in \mathbb{C}$. For the cases (a) $N = 15$, $\theta_2 = 15^\circ$ and (b) $N = 10$, $\theta_2 = 30^\circ$, the spatial-correlations $\cos(\boldsymbol{s}_0, \boldsymbol{s}_2)$ are approximately given by (a) 0.656 and (b) -0.13, respectively. This implies that $\boldsymbol{s}_0$ is far from orthogonal to $\boldsymbol{s}_2$ in (a), while almost orthogonal in (b). Hence, $\boldsymbol{s}_0$ is also far from orthogonal to $\boldsymbol{y}(n)$ in (a), which is true especially when the power of spatially-correlated interference is high.

Based on this consideration, Fig. 3 illustrates a geometric interpretation of CNLMS and PNLMS ($\lambda_n = 1$) in (a) spatially-correlated and (b) spatially-uncorrelated cases. As we can see, $\boldsymbol{w}_n^{(\mathrm{C})}$ moves to the intersection $H_n \cap K$ along the constraint K without stepping away, whereas $\boldsymbol{w}_n^{(\mathrm{P})}$ moves to H_n and then goes back to K. Thus, CNLMS and PNLMS are called *embedded-constraint* and *non-embedded-constraint*, respectively, since the constraint is embedded in the direction of update for CNLMS (and *not* for PNLMS). We observe that PNLMS obtains a point far from the intersection $H_n \cap K$ especially in the case (a), while CNLMS obtains the projection onto the intersection in the both

[2] In [3], the method is called normalized OPM based gradient projection (OPM-GP), which is indeed a normalized version of the method in [2].

cases. Hence, assuming $\boldsymbol{w}_{\rm opt} \in H_n \cap K$, an advantage of CNLMS over PNLMS in convergence speed is naturally expected (see Fig. 1). *The spatial-correlation should be the key factor that governs the extent of the difference in convergence speed between CNLMS and PNLMS.*

From the above discussion, it is of great interest to develop an efficient embedded-constraint beamformer by devising the CNLMS algorithm for further acceleration. In the following subsection, we propose a novel embedded-constraint adaptive beamformer based on the constrained parallel projection.

3.2. Proposed Embedded-Constraint Adaptive Beamformer

In Sec. 2, the linearly constrained narrowband beamforming problem is defined in the complex-valued vector space $\mathcal{H}_{\mathbb{C}}(:= \mathbb{C}^N)$. We can equivalently reformulate the problem in a real-valued vector space $\mathcal{H}_{\mathbb{R}}(:= \mathbb{R}^{2N})$ by a bijective mapping between $\mathcal{H}_{\mathbb{R}}$ and $\mathcal{H}_{\mathbb{C}}$ (so that we can directly utilize the results in [15, 16]).

For any $\boldsymbol{v} = \boldsymbol{v}_R + i\boldsymbol{v}_I \in \mathcal{H}_{\mathbb{C}}$ ($\boldsymbol{v}_R, \boldsymbol{v}_I \in \mathbb{R}^N$), let $\widehat{\boldsymbol{v}} := [\boldsymbol{v}_R^T, \boldsymbol{v}_I^T]^T \in \mathcal{H}_{\mathbb{R}}$, where the subscripts R and I respectively stand for the real and imaginary parts of a scalar/vector/matrix. Similarly, for any set $S \subset \mathcal{H}_{\mathbb{C}}$, define $\widehat{S} := \{\widehat{\boldsymbol{v}} = [\boldsymbol{v}_R^T, \boldsymbol{v}_I^T]^T : \boldsymbol{v}_R + i\boldsymbol{v}_I \in S\} \subset \mathcal{H}_{\mathbb{R}}$. Given $\boldsymbol{a}, \boldsymbol{b} \in \mathcal{H}_{\mathbb{C}}$, the following hold: $\langle \boldsymbol{a}, \boldsymbol{b}\rangle_R = \widehat{\boldsymbol{a}}^T\widehat{\boldsymbol{b}}$, $\langle \boldsymbol{a}, \boldsymbol{b}\rangle_I = \widehat{\boldsymbol{a}}^T\boldsymbol{B}\widehat{\boldsymbol{b}}$, where $\boldsymbol{B} := \begin{bmatrix} \boldsymbol{0} & \boldsymbol{I}_N \\ -\boldsymbol{I}_N & \boldsymbol{0} \end{bmatrix} \in \mathbb{R}^{2N\times 2N}$ ($\boldsymbol{I}_N$: $N\times N$ identity matrix). The linearly constrained narrowband beamforming problem is formulated in $\mathcal{H}_{\mathbb{R}}$ as follows:

$$\text{find } \widehat{\boldsymbol{w}}_{\rm opt} \in \arg \min_{\widehat{\boldsymbol{z}} \in \widehat{K}(\boldsymbol{A},\boldsymbol{b})} \widehat{\boldsymbol{z}}^T \widehat{\boldsymbol{R}}_{\boldsymbol{y}} \widehat{\boldsymbol{z}}, \tag{3}$$

where $\widehat{\boldsymbol{R}}_{\boldsymbol{y}} := \begin{bmatrix} (\boldsymbol{R}_{\boldsymbol{y}})_R & -(\boldsymbol{R}_{\boldsymbol{y}})_I \\ (\boldsymbol{R}_{\boldsymbol{y}})_I & (\boldsymbol{R}_{\boldsymbol{y}})_R \end{bmatrix}$. We remark that $\widehat{\boldsymbol{z}}^T \widehat{\boldsymbol{R}}_{\boldsymbol{y}} \widehat{\boldsymbol{z}} = E\left\{\left\|[\widehat{\boldsymbol{y}}(\iota), \boldsymbol{B}\widehat{\boldsymbol{y}}(\iota)]^T \widehat{\boldsymbol{z}}\right\|^2\right\}$. The constraint set $K \subset \mathcal{H}_{\mathbb{C}}$ is equivalently mapped to

$$\widehat{K} := \{\widehat{\boldsymbol{z}} \in \mathcal{H}_{\mathbb{R}} : [\widehat{\boldsymbol{s}}_0, \boldsymbol{B}\widehat{\boldsymbol{s}}_0]^T \widehat{\boldsymbol{z}} = [1, 0]^T\} \subset \mathcal{H}_{\mathbb{R}}.$$

Our approach is based on the *set-theoretic* adaptive filtering framework [15–17]. The optimal beamformer $\widehat{\boldsymbol{w}}_{\rm opt} \in \mathcal{H}_{\mathbb{R}}$ is approximated as a point in the intersection of certain closed convex sets defined by the received signals (and possibly a priori information). At each iteration, different convex sets are defined and the distance to their intersection is reduced monotonically. The desirable properties for the convex sets are (i) to contain $\widehat{\boldsymbol{w}}_{\rm opt}$ with high reliability for *stable convergence* and (ii) to have a fairly small intersection for *fast convergence*. Our strategy is to appropriately inflate the sets for (i) and utilize multiple convex sets at each iteration for (ii).

At each iteration $n \in \mathbb{N}^*$, the multiple closed convex sets $\widehat{C}_\iota(\rho_n)$ are defined by the multiple received vectors $\widehat{\boldsymbol{y}}(\iota)$, $\forall \iota \in \mathcal{I}_n := \{n, n-1, \cdots, \max\{1, n-q+1\}\}$, where $q \in \mathbb{N}^*$. Namely, we use the data observed at the last $\min\{q, n\}$ snapshots. Based on the remark under (3), we define the stochastic property sets as follows:

$$\widehat{C}_\iota(\rho_n) := \left\{\widehat{\boldsymbol{z}} \in \mathcal{H}_{\mathbb{R}} : \left\|[\widehat{\boldsymbol{y}}(\iota), \boldsymbol{B}\widehat{\boldsymbol{y}}(\iota)]^T \widehat{\boldsymbol{z}}\right\|^2 \leq \rho_n\right\}, \forall \iota \in \mathcal{I}_n,$$

which is equivalently represented in $\mathcal{H}_{\mathbb{C}}$ as $C_\iota(\rho_n) := \{\boldsymbol{z} \in \mathcal{H}_{\mathbb{C}} : |\langle \boldsymbol{y}(\iota), \boldsymbol{z}\rangle|^2 \leq \rho_n\}, \forall \iota \in \mathcal{I}_n$. Here, ρ_n, $\forall n \in \mathbb{N}^*$, is a positive constant governing the reliability such that $\widehat{\boldsymbol{w}}_{\rm opt} \in \widehat{C}_\iota(\rho_n)$. A simple design of ρ_n is $\rho_n = 0$, $\forall n \in \mathbb{N}^*$, as in CNLMS, which utilizes $P_{\widehat{C}_n(0)\cap\widehat{K}}(\widehat{\boldsymbol{w}}_n)$. Another simple design will be an estimate of $E\{|\langle \boldsymbol{y}(n), \boldsymbol{w}_{\rm opt}\rangle|^2\} = E\{\|[\widehat{\boldsymbol{y}}(n), \boldsymbol{B}\widehat{\boldsymbol{y}}(n)]^T \widehat{\boldsymbol{w}}_{\rm opt}\|^2\}$ as shown below.

Example 1 *Given the initial value $\rho_0 = 0$ and the exponential factor $\gamma \in [0, 1]$, generate a sequence $(\rho_n)_{n\in\mathbb{N}^*}$ recursively as $\rho_n = \gamma\rho_{n-1} + (1-\gamma)\left\|[\widehat{\boldsymbol{y}}(n), \boldsymbol{B}\widehat{\boldsymbol{y}}(n)]^T \widehat{\boldsymbol{w}}_n\right\|^2$.*

To extend the embedded-constraint algorithm in [9] to complex cases in a computationally-efficient manner, $P_{\widehat{C}_\iota(\rho_n)\cap\widehat{K}}(\widehat{\boldsymbol{w}}_n)$, $\iota \in \mathcal{I}_n$, should simply be computed (see also Algorithms in Sec. 3.1). Fortunately, we can derive the following simple formula.

Proposition 1 *Suppose that $\widehat{C}_\iota(\rho_n) \cap \widehat{K} \neq \emptyset$ for $\iota \in \mathcal{I}_n$ and $n \in \mathbb{N}^*$. Let $\boldsymbol{y}_r(\iota) := e^{-i\alpha_n(\iota)}\boldsymbol{y}(\iota)$ with $\alpha_n(\iota) := \angle\langle \boldsymbol{y}(\iota), \boldsymbol{w}_n\rangle$. Then, we obtain*

$$P_{\widehat{C}_\iota(\rho_n)\cap\widehat{K}}(\widehat{\boldsymbol{w}}_n) = \begin{cases} \widehat{\boldsymbol{w}}_n - \dfrac{\widehat{\boldsymbol{y}}_r^T(\iota)\widehat{\boldsymbol{w}}_n - \sqrt{\rho_n}}{\widehat{\boldsymbol{y}}_r^T(\iota)\boldsymbol{Q}\widehat{\boldsymbol{y}}_r(\iota)}\boldsymbol{Q}\widehat{\boldsymbol{y}}_r(\iota), \\ \text{if } \widehat{\boldsymbol{w}}_n \notin \widehat{C}_\iota(\rho_n), \\ \widehat{\boldsymbol{w}}_n, \quad \text{otherwise}, \end{cases} \tag{4}$$

where $\boldsymbol{Q} := \boldsymbol{I}_{2N} - [\widehat{\boldsymbol{s}}_0, \boldsymbol{B}\widehat{\boldsymbol{s}}_0][\widehat{\boldsymbol{s}}_0, \boldsymbol{B}\widehat{\boldsymbol{s}}_0]^T$ is the projection matrix onto $\widehat{M}$, the translated subspace of $\widehat{K}$.

Proof is omitted. The proposed beamformer is given as follows.

Algorithm 1 *With an initial estimate $\widehat{\boldsymbol{w}}_0 := \widehat{\boldsymbol{s}}_0 \in \widehat{K}$, generate iteratively a sequence of beamforming vectors $(\widehat{\boldsymbol{w}}_n)_{n\in\mathbb{N}^*}$ by*

$$\widehat{\boldsymbol{w}}_{n+1} = \widehat{\boldsymbol{w}}_n + \lambda_n\mathcal{M}_n\left(\sum_{\iota\in\mathcal{I}_n}\omega_\iota^{(n)}P_{\widehat{C}_\iota(\rho_n)\cap\widehat{K}}(\widehat{\boldsymbol{w}}_n) - \widehat{\boldsymbol{w}}_n\right), \tag{5}$$

$\forall n \in \mathbb{N}^*$, where $\lambda_n \in [0, 2]$, $\omega_\iota^{(n)} \in (0, 1]$, $\forall \iota \in \mathcal{I}_n$, is the weight satisfying $\sum_{\iota\in\mathcal{I}_n}\omega_\iota^{(n)} = 1$, and

$$\mathcal{M}_n := \begin{cases} \dfrac{\sum_{\iota\in\mathcal{I}_n}\omega_\iota^{(n)}\left\|P_{\widehat{C}_\iota(\rho_n)\cap\widehat{K}}(\widehat{\boldsymbol{w}}_n) - \widehat{\boldsymbol{w}}_n\right\|^2}{\left\|\sum_{\iota\in\mathcal{I}_n}\omega_\iota^{(n)}P_{\widehat{C}_\iota(\rho_n)\cap\widehat{K}}(\widehat{\boldsymbol{w}}_n) - \widehat{\boldsymbol{w}}_n\right\|^2}, \\ \qquad \text{if } \widehat{\boldsymbol{w}}_n \notin \bigcap_{\iota\in\mathcal{I}_n}\widehat{C}_\iota(\rho_n) \cap \widehat{K}, \\ 1, \qquad \text{otherwise}. \end{cases}$$

If $\widehat{C}_\iota(\rho_n) \cap \widehat{K} = \emptyset$, $P_{\widehat{C}_\iota(\rho_n)\cap\widehat{K}}(\widehat{\boldsymbol{w}}_n)$ is not defined. Fortunately, we have $\widehat{C}_\iota(\rho_n) \cap \widehat{K} = \emptyset \Leftrightarrow \begin{cases} \widehat{\boldsymbol{y}}(\iota) \in \text{span}\{\widehat{\boldsymbol{s}}_0, \boldsymbol{B}\widehat{\boldsymbol{s}}_0\} \text{ and} \\ \|\widehat{\boldsymbol{y}}(\iota)\| > \rho_n\|\widehat{\boldsymbol{s}}_0\|, \end{cases}$ which happens only when interferences plus noise is spatially-correlated with SOI completely. In such an extreme case, there is nothing for a beamformer to do, thus $P_{\widehat{C}_\iota(\rho_n)\cap\widehat{K}}(\widehat{\boldsymbol{w}}_n)$ is simply replaced by $\widehat{\boldsymbol{w}}_n$.

By assigning $q = 1$ and $\rho_n = 0, \forall n \in \mathbb{N}^*$, we have $\mathcal{M}_n = 1$, $\forall n \in \mathbb{N}^*$, thus (5) gives the equivalent real-vector expression of the complex vector version of the CNLMS algorithm (see Algorithms in Sec. 2). The update equation in (5) is called the *constrained parallel projection* (see [9, AppendixD]). The computational complexity issue is discussed in the concluding remarks.

4. SIMULATIONS AND CONCLUDING REMARKS

To demonstrate the efficacy of the proposed beamformer, simulations are performed under exactly the same conditions as in Fig. 1 (see Sec. 3.1). In the case (a), we set the parameters as follows: $\lambda_n = 0.02$ for CNLMS [4]; $r = 2$ (r: affine dimension), $\lambda_n = 0.008$ for the constrained affine projection algorithm (CAPA)-a [5]; $r = 5$, $\lambda_n = 0.005$ for CAPA-b; $q = 20$, $\lambda_n = 0.004, 0.0015$ for Proposed-a and Proposed-b, respectively. We use ρ_n presented in Example 1 with $\gamma = 0.999$ for proposed-a,

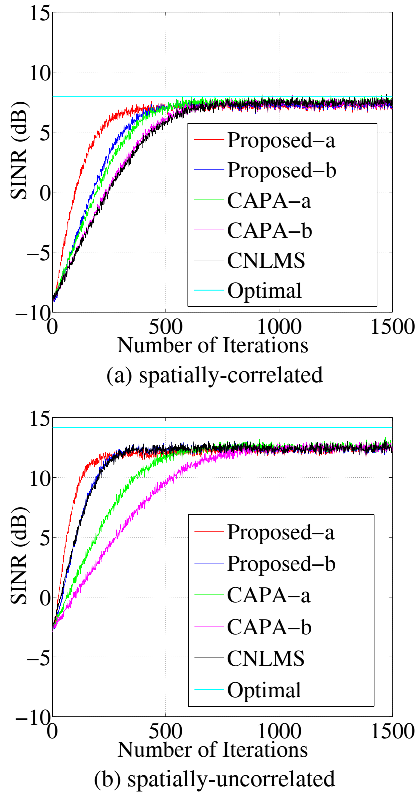

Fig. 4. SINR curve: proposed versus CAPA and CNLMS.

and $\rho_n = 0$, $\forall n \in \mathbb{N}^*$, for proposed-b. In the case (b), we set as follows: $\lambda_n = 0.0055$ for CAPA-a; $\lambda_n = 0.0035$ for CAPA-b; $\lambda_n = 0.0025, 0.0011$ for Proposed-a and Proposed-b [the others are the same as in (a)]. The step size for each algorithm is carefully tuned so that all algorithms achieve the same SINR level in steady-state. The results are drawn in Fig. 4. We observe that the proposed beamformer attains a remarkable gain in convergence speed compared with CAPA and CNLMS especially in the case (a).

CONCLUDING REMARKS

From our extensive experiments, we conclude that the proposed beamformer is effective especially in the presence of spatially-correlated interferences. We remark that the proposed beamformer exhibits superiority to CAPA and CNLMS among all our experiments, while CAPA sometimes exhibits inferiority to CNLMS, as shown in Fig. 4. This stems from the noise sensitivity of APA [17].

The proposed beamformer has a notable advantage in terms of saving time consumption, because each projection in (5) can be computed in parallel by employing concurrent processors. With such processors, the computational complexity imposed on each processor is kept $O(N)$. Note that the computation of $\boldsymbol{Q}\widehat{\boldsymbol{y}}_r(\iota) = \widehat{\boldsymbol{y}}_r(\iota) - \langle \widehat{\boldsymbol{s}}_0, \widehat{\boldsymbol{y}}_r(\iota)\rangle \widehat{\boldsymbol{s}}_0 - \langle \boldsymbol{B}\widehat{\boldsymbol{s}}_0, \widehat{\boldsymbol{y}}_r(\iota)\rangle \boldsymbol{B}\widehat{\boldsymbol{s}}_0$ in (4) just requires $4N$ multiplications. Moreover, even if some of the engaged processors are damaged, the proposed beamformer can update the weight vector based on information computed by the other processors with just a slight loss in convergence speed, which implies that the algorithm is endowed with a fault-tolerance nature.

For saving power consumption, it will be a good strategy to switch the proposed and CNLMS algorithms ($q = 1$ and $\rho_n = 0$ in Algorithm 1) based on spatial-correlation between SOI and interferences. To attain information about the spatial-correlation, we can utilize a recently established technique [18] (based on *algebraic phase unwrapping*) which directly counts the number of signals arriving from an arbitrary range of direction without estimating the exact DOA of the signals.

Acknowledgment: The authors would like to express their deep gratitude to Prof. K. Sakaniwa of Tokyo Institute of Technology for fruitful discussions. This work was supported in part by JSPS Grants-in-Aid (178440).

5. REFERENCES

[1] O. L. Frost, "An algorithm for linearly constrained adaptive array processing," in *Proc. IEEE*, 1972, vol. 60, pp. 926–935.

[2] M. Honig, U. Madhow, and S. Verdu, "Blind adaptive multiuser detection," *IEEE Trans. Inform. Theory*, vol. 41, no. 4, pp. 944–960, July 1995.

[3] S. C. Park and J. F. Doherty, "Generalized projection algorithm for blind interference suppression in DS/CDMA communications," *IEEE Trans. Circuits and Syst.–II*, vol. 44, no. 6, pp. 453–460, June 1997.

[4] J. A. Apolinário Jr., S. Werner, P. S. R. Diniz, and T. I. Laakso, "Constrained normalized adaptive filters for CDMA mobile communications," in *Proc. EUSIPCO*, 1998, vol. IV, pp. 2053–2056.

[5] M. L. R. de Campos, J. Antonio, and J. A. Apolinário Jr., "The constrained affine projection algorithm —Development and convergence issues," in *Proc. 1st Balkan Conf. on Signal Processing, Commun., Circuits and Syst.*, 2000, Turkey.

[6] M. L. R. de Campos, S. Werner, and J. A. Apolinário Jr., "Constrained adaptation algorithms employing householder transformation," *IEEE Trans. Signal Processing*, vol. 50, no. 9, pp. 2187–2195, Sept. 2002.

[7] H. L. Van Trees, *Optimum array processing —Part IV of Detection, Estimation, and Modulation Theory*, New York: Wiley, 2002.

[8] R. L. G. Cavalcante, I. Yamada, and K. Sakaniwa, "A fast blind MAI reduction based on adaptive projected subgradient method," *IEICE Trans. Fundamentals*, vol. E87-A, no. 8, pp. 1973–1980, Aug. 2004.

[9] M. Yukawa, R. L. G. Cavalcante, and I. Yamada, "Efficient blind MAI suppression in DS/CDMA systems by embedded constraint parallel projection techniques," *IEICE Trans. Fundamentals*, vol. E88-A, no. 8, pp. 2062–2071, Aug. 2005.

[10] M. Wax and Y. Anu, "Performance analysis of the minimum variance beamformer," *IEEE Trans. Signal Processing*, vol. 44, no. 4, pp. 928–937, Apr. 1996.

[11] Y. Bresler, V. U. Reddy, and T. Kailath, "Optimum beamformer for coherent signal and interferences," *IEEE Trans. Acoust., Speech, Signal Processing*, vol. 36, no. 6, pp. 833–843, June 1988.

[12] H. Clergeot, A. Ouamri, and S. Tressens, "High resolution spectral method for spatial discrimination of closely spaced correlated sources," in *Proc. IEEE ICASSP*, 1985, vol. 10, pp. 560–563.

[13] R. L. G. Cavalcante, M. Yukawa, and I. Yamada, "Set-theoretic DS/CDMA receivers for fading channels by adaptive projected subgradient method," in *Proc. IEEE GLOBECOM*, St. Louis, MA, 2005.

[14] L. B. Fertig and J. H. McClellan, "Dual forms for constrained adaptive filtering," *IEEE Trans. Signal Processing*, vol. 42, no. 1, pp. 11–23, Jan. 1994.

[15] I. Yamada, "Adaptive projected subgradient method: A unified view for projection based adaptive algorithms," *The Journal of IEICE*, vol. 86, no. 8, pp. 654–658, Aug. 2003, in Japanese.

[16] I. Yamada and N. Ogura, "Adaptive projected subgradient method for asymptotic minimization of sequence of nonnegative convex functions," *Numer. Funct. Anal. Optim.*, vol. 25, no. 7&8, pp. 593–617, 2004.

[17] I. Yamada, K. Slavakis, and K. Yamada, "An efficient robust adaptive filtering algorithm based on parallel subgradient projection techniques," *IEEE Trans. Signal Processing*, vol. 50, no. 5, pp. 1091–1101, 2002.

[18] I. Yamada, "High-resolution DOA estimation by algebraic phase unwrapping algorithm," in *Proc. IEEE ISCAS*, 2005.